

# Reversal of Blindness in Animal Models of Leber Congenital Amaurosis Using Optimized AAV2-mediated Gene Transfer

Jeannette Bennicelli<sup>1</sup>, John Fraser Wright<sup>2,3</sup>, Andras Komaromy<sup>4</sup>, Jonathan B Jacobs<sup>5</sup>, Bernd Hauck<sup>2</sup>, Olga Zelenai<sup>2</sup>, Federico Mingozzi<sup>2</sup>, Daniel Hui<sup>2</sup>, Daniel Chung<sup>1</sup>, Tonia S Rex<sup>1</sup>, Zhangyong Wei<sup>1</sup>, Guang Qu<sup>2</sup>, Shangzhen Zhou<sup>2</sup>, Caroline Zeiss<sup>6,7</sup>, Valder R Arruda<sup>2</sup>, Gregory M Acland<sup>8</sup>, Lou F Dell'Osso<sup>5</sup>, Katherine A High<sup>2</sup>, Albert M Maguire<sup>1</sup> and Jean Bennett<sup>1</sup>

<sup>1</sup>Department of Ophthalmology, Scheie Eye Institute, University of Pennsylvania, Philadelphia, Pennsylvania, USA; <sup>2</sup>Center for Cellular and Molecular Therapy (CCMT), Children's Hospital of Philadelphia, Philadelphia, Pennsylvania, USA; <sup>3</sup>Department of Pathology and Laboratory Medicine, University of Pennsylvania, Philadelphia, Pennsylvania, USA; <sup>4</sup>School of Veterinary Medicine, University of Pennsylvania, Philadelphia, Pennsylvania, USA; <sup>5</sup>Darof-Dell'Osso Ocular Motility Lab, LSC DVA Medical School and CASE Medical School, Case Western Reserve University, Cleveland, Ohio, USA; <sup>6</sup>Section of Comparative Medicine, Yale School of Medicine, New Haven, Connecticut, USA; <sup>7</sup>Department of Ophthalmology and Visual Science, Yale School of Medicine, New Haven, Connecticut, USA; <sup>8</sup>Baker Institute, College of Veterinary Medicine, Cornell University, Ithaca, New York, USA

We evaluated the safety and efficacy of an optimized adeno-associated virus (AAV; AAV2.*RPE65*) in animal models of the *RPE65* form of Leber congenital amaurosis (LCA). Protein expression was optimized by addition of a modified Kozak sequence at the translational start site of hRPE65. Modifications in AAV production and delivery included use of a long stuffer sequence to prevent reverse packaging from the AAV inverted-terminal repeats, and co-injection with a surfactant. The latter allows consistent and predictable delivery of a given dose of vector. We observed improved electroretinograms (ERGs) and visual acuity in *Rpe65* mutant mice. This has not been reported previously using AAV2 vectors. Subretinal delivery of  $8.25 \times 10^{10}$  vector genomes in affected dogs was well tolerated both locally and systemically, and treated animals showed improved visual behavior and pupillary responses, and reduced nystagmus within 2 weeks of injection. ERG responses confirmed the reversal of visual deficit. Immunohistochemistry confirmed transduction of retinal pigment epithelium cells and there was minimal toxicity to the retina as judged by histopathologic analysis. The data demonstrate that AAV2.*RPE65* delivers the *RPE65* transgene efficiently and quickly to the appropriate target cells *in vivo* in animal models. This vector holds great promise for treatment of LCA due to *RPE65* mutations.

Received 13 June 2007; accepted 27 November 2007; advance online publication 22 January 2008. doi:10.1038/sj.mt.6300389

## INTRODUCTION

Leber congenital amaurosis (LCA) is an incurable group of childhood-onset genetic retinal degenerative diseases, which can arise from mutations in any one of at least nine different

genes (<sup>1-6</sup>, <http://www.sph.uth.tmc.edu/RetNet>). The form of LCA caused by mutations in the *RPE65* gene is an ideal target for development of therapies because this form of the disease accounts for ~20% of disease in the human population; the normal distribution and function of the *RPE65* gene is understood, and there are several animal models, including both genetically engineered and spontaneous mutant mice and naturally occurring canine models.<sup>7-11</sup>

The initial studies demonstrating restoration of vision through gene augmentation therapy were reported in the canine model of *RPE65*-associated LCA.<sup>8</sup> Additional reports have confirmed the success of the treatment in a larger number of dogs using adeno-associated virus 2 (AAV2) vectors.<sup>7,12,13</sup> This study was designed to (i) optimize specific features of the transgene cassette, virus, and excipient for efficient transduction of retinal pigment epithelium (rpe), and (ii) provide additional detail relating to time of onset of visual improvement and the stability of this effect over a 3-month period in a large animal model using optimized conditions. In addition, treatment-associated toxicity was monitored. The results show evidence of therapeutic effect in mouse models in which such a response was lacking using previous versions of AAV2 to deliver *RPE65*.<sup>14,15</sup> Therapeutic effect, including reversal of afferent pupillary defects, nystagmus, retinal and visual function was also observed within 2–5 weeks of treatment in the canine model and was sustained over a 3-month period. The data demonstrate the high level of efficacy and minimal toxicity of the vector and treatment paradigm.

## RESULTS

### Vector and vector recovery from administration devices

The transgene in AAV2.*RPE65* consists of the 1.6-kilo base (kb) human *RPE65* complementary DNA (cDNA)<sup>7,8,15</sup> with a

The first two authors contributed equally to this work.

Correspondence: Jean Bennett, F.M. Kirby Center for Molecular Ophthalmology, Scheie Eye Institute, University of Pennsylvania, 309C Stellar-Chance Labs, 422 Curie Boulevard, Philadelphia, Pennsylvania 19104-6069, USA. E-mail: [jebennet@mail.med.upenn.edu](mailto:jebennet@mail.med.upenn.edu)

modified Kozak sequence engineered at the translational start site. The cDNA is under control of a hybrid chicken  $\beta$ -actin (CBA) promoter. A long (6.9 kb) stuffer sequence was included to prevent reverse packaging (*i.e.*, of non-transgene containing) vector from the AAV inverted-terminal repeats.

Vector recovery was assessed in the presence or absence of the surfactant Pluronic F68 (PF68) following vector dilution and passage through injection devices. As shown in **Figure 1a**, stock AAV2.*RPE65* vector diluted to a target concentration of  $1 \times 10^{11}$  vector genomes (vg)/ml either supplemented (+PF68) or not (-PF68) with 0.001% PF68 and then passed through device A, was recovered at  $106.8\% \pm 9.3\%$  and  $50.9\% \pm 6.0\%$ , respectively. The vector, similarly diluted and passed through device B, resulted in an average recovery of  $104.3\% \pm 7.0\%$  when PF68 was present and  $23.7\% \pm 4.8\%$  in the absence of the surfactant. For device C, average vector recoveries were  $94.1\% \pm 5.5\%$  and  $27.5\% \pm 7.4\%$  in the presence or absence, respectively, of PF68. These results indicated that the surfactant was required to achieve consistent and quantitative recovery of the vector, diluted to concentrations relevant to animal models and prospective clinical studies.

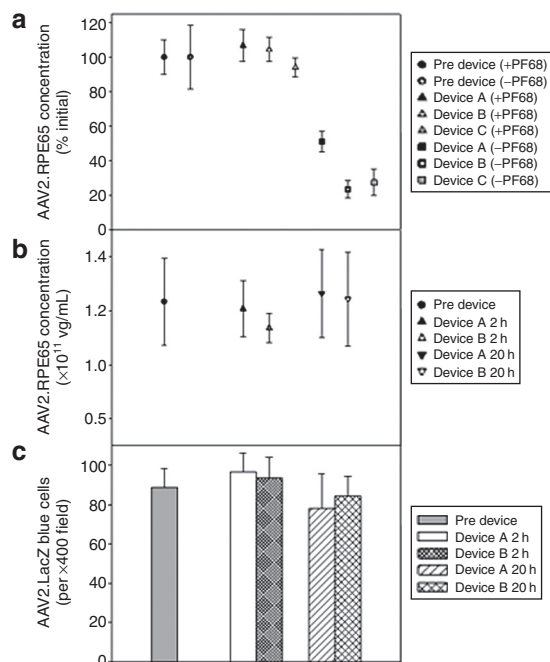


**Figure 1** Recovery of adeno-associated virus 2 (AAV2) vector following dilution and passage through administration devices. **(a)** Stock AAV2.*RPE65* vector diluted to a target working concentration of  $1 \times 10^{11}$  vector genome (vg)/ml in phosphate-buffered saline (PBS) supplement (+PF68) or not (-PF68) with Pluronic F68 (PF68) (0.001%) was drawn into 1-mL syringes, vector was passed through device A, B or device C, and the concentration of recovered vector was measured by quantitative-polymerase chain reaction (Q-PCR). **(b)** AAV2.*RPE65* vector diluted to a target working concentration of  $1 \times 10^{11}$  vg/ml in PBS supplemented with PF68 (0.001%) was drawn into 1-ml syringes, incubated for 2 or 20 hours, then passed through device A or device B, and the concentration of recovered vector measured by Q-PCR. **(c)** AAV2.*LacZ* vector subjected to the same procedure described for AAV2.*RPE65* in **b** was tested for transduction titer as described in Materials and Methods. Quantitative post-device recovery of vector titer and functional activity provide assurance of consistent vector dosing under conditions of immediate or delayed use that may occur in a surgical suite.

A second study was performed to further characterize vector recovery using the optimized PBS180 + 0.001% PF68 formulation in devices A and B, by evaluation of the effect of extended incubation time in devices on vector genome titer recovery using AAV2.*RPE65*, and evaluation of functional activity using AAV2.*LacZ* vector as a surrogate. As shown in **Figure 1b**, the recovery of AAV2.*RPE65* vector after a 2-hour [ $1.21 \pm 0.10$  (SD)  $\times 10^{11}$  vg/ml] or 20-hour ( $1.26 \pm 0.16 \times 10^{11}$  vg/ml) storage, and passage through device A was not significantly different from the concentration in the pre-device vector dilution ( $1.23 \pm 0.16 \times 10^{11}$  vg/ml). Similarly, the recovery of vector after a 2-hour ( $1.14 \pm 0.06 \times 10^{11}$  vg/ml) or 20-hour ( $1.24 \pm 0.17 \times 10^{11}$  vg/ml) storage and passage through device B was not significantly different from the pre-device vector concentration. AAV2.*LacZ* similarly diluted to a target concentration of  $1 \times 10^{11}$  vg/ml in PBS180 + PF68, stored and then passed through devices A and B, was evaluated for transduction titer following ejection from the devices. As shown in **Figure 1c**, compared with the starting material ( $88.7 \pm 9.6$  blue cells/field), there was no significant loss of transduction titer after a 2-hour ( $96.7 \pm 9.4$  blue cells/field) or 20-hour ( $78 \pm 17.6$  blue cells/field) incubation and passage through device A. Similarly, no significant change was observed following 2-hour ( $93.5 \pm 10.7$  blue cells/field) or 20-hour ( $84.2 \pm 10.4$  blue cells/field) using device B.

Vector infectivity was also assessed before and after AAV2.*RPE65* storage for 2 hours and then passage through devices A or B. Recovery from both devices was 25 vg/IU, not significantly different from the infectivity titer of 31 vg/IU measured for the same vector unexposed to the devices.

Together these data demonstrate that the PBS180 + PF68 vector formulation enabled quantitative recovery of vector genome titer and functional activity of dilute AAV2 vector solutions following handling manipulations, incubation at room temperature for up to 20 hours, and passage through vector administration devices.

## Animal studies

**Mice.** Unilateral subretinal injections of  $1 \times 10^9$  AAV2.*RPE65* were performed in cohorts of 10 *Rpe65* knockout (*Rpe65*<sup>-/-</sup>) mice, aged 1–2 months. Contralateral eyes were subjected to a sham injection. *Rpe65*<sup>-/-</sup> mice have not yet been shown to respond to AAV2/2-mediated delivery of *RPE65*.<sup>14</sup> Electroretinograms (ERGs) were carried out to identify any improvement in retinal function 3–4 weeks after injection.

Waveforms of untreated or sham-injected *Rpe65*<sup>-/-</sup> mice were essentially flat. In contrast, there were improved waveforms and amplitudes in the AAV2.*RPE65*-treated eyes in 4 of the 10 mice. Improvements were observed in both the scotopic  $b_{max}$  and the rod and cone photoreceptor  $a_{max}$ . The amplitude of waves increased significantly from 0 (untreated or control-injected *Rpe65*<sup>-/-</sup> mice) to 189  $\mu$ V, which is twofold lower than those of wild-type C57Bl/6 mice. Improvements were also noted in b waves of eyes of *Rpe65*<sup>-/-</sup> mice treated with AAV2.*RPE65*, with average b-wave amplitudes of 0.5  $\mu$ V for untreated *Rpe65*<sup>-/-</sup> mice, 59  $\mu$ V for treated *Rpe65*<sup>-/-</sup> mice, and 233  $\mu$ V for C57Bl/6 control eyes. Animals were killed and eyes harvested immediately after the ERG recordings. The *RPE65* protein was identified

immunohistochemically in rpe cells only in eyes exposed to AAV2.*RPE65* (data not shown). In one eye, RPE65 protein was also detected in ganglion cells.

Similar reversals of ERG deficits were obtained using *rd12* (*Rpe65* spontaneous null) mice. In these animals, acuity measurements were also made. Those demonstrated significant improvements in acuity in the eyes treated subretinally with AAV2.*RPE65* (Figure 2a). Consistent with the improvements in retinal and visual function, RPE65 protein was found localized to the rpe cells, but not other retinal cell types, in the injected eyes (Figure 2b). RPE65 protein was absent in untreated or sham-injected eyes (Figure 2c).

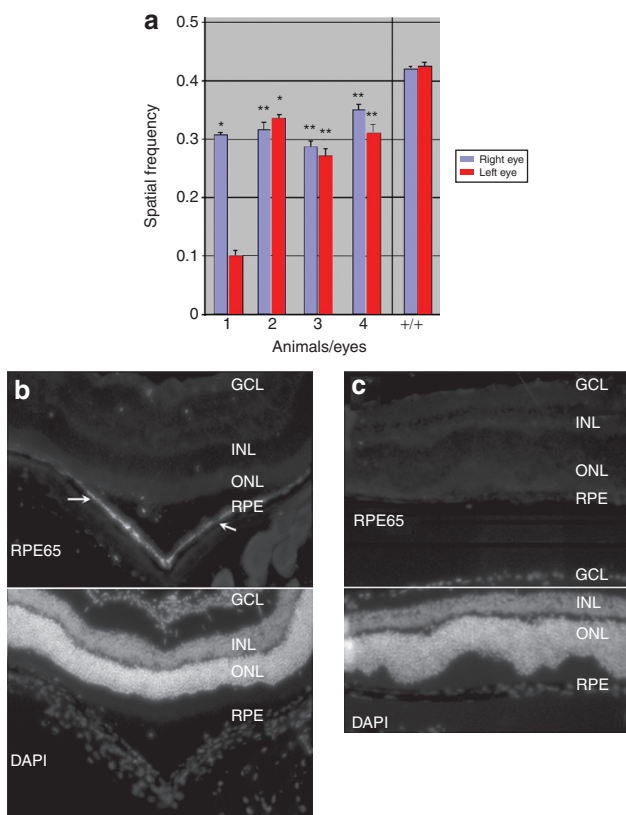


**Figure 2** Improvement in visual acuity in mice correlates with immunohistochemical localization of RPE65 in Rpe cells after subretinal injection with AAV2-*RPE65*. (a) Post-treatment optokinetic (Optomotry) responses of treated and control eyes of four *rd12* (*Rpe65* null) mice and of a control (phenotypically normal) C57Bl/6 mouse. There is significant improvement in visual acuity in eyes of all *rd12* mice injected subretinally with AAV2-*RPE65* compared with the control eye (left eye of animal 1). \* $P \leq 0.005$ ; \*\* $P \leq 0.02$ . Testing was performed 1 month post-injection. The experimenter was unaware of the age, and treatment paradigm of the tested animals and the direction of rotation of the sinusoidal pattern presented to the animal. Mice were tested under photopic conditions during their daytime light cycle and four separate trials were performed per animal. RPE65 protein is detectable by immunohistochemistry in (b) the rpe (only) of the right, subretinally injected eye, but not in (c) the contralateral, uninjected (control) eye. These are the eyes from animal #1, shown in a. Upper panels in b and c show RPE65-specific fluorescence (arrows); lower panels show 4,6-diamidino-2-phenylindole (DAPI) fluorescence. Immunohistochemistry was performed 1 month post-injection. GCL, ganglion cell layer; INL, inner nuclear layer; ONL, outer nuclear layer; RPE, retinal pigment epithelium.

**Dogs.** Three *RPE65* mutant dogs were evaluated prior to treatment for presence and type of nystagmus. One of the animals was found to have large amplitude, classic infantile nystagmus waveforms, including pendular and jerk movements in both the horizontal and vertical planes. This prevented the dog from keeping visual targets within the area centralis (the region of highest receptor density, spanning  $+3^\circ$  horizontally by  $+1.5^\circ$  vertically, analogous to the fovea). The other two had steady gaze. Five eyes of the three *RPE65* mutant dogs were injected when the dogs were 3.5 months old with  $8.25 \times 10^{10}$  vg AAV2.*RPE65* subretinally and the sixth eye received an intravitreal injection of the same dose. Virus was delivered in phosphate-buffered saline (PBS) in the presence or absence of 0.001% PF68. (Table 1; Supplementary Figure S1). Injections were administered without complication except for an inadvertent choroidal injury during injection of BR332, in the right eye. All subretinally injected retinas reattached spontaneously within days after injection and ocular media were clear.

Animals were evaluated at weekly intervals for the first month following injection for alterations in pupillary responses, and nystagmus. By 2 weeks post-treatment, improvements in pupillary responses, nystagmus, and visual behavior were noted (Supplementary Figure S2). These continued to improve through the 1-month timepoint.

Repeat detailed ocular motility characterizations were measured at the 4-week timepoint. Figure 3 shows the nystagmus waveforms of both eyes of dog BR334 (Figure 3a) prior to and (Figure 3b) after subretinal injection of one eye. Before treatment, nystagmus was present in both eyes with comparable characteristics. By 1 month post-treatment (Figure 3b), there was significant diminution of abnormal movement in both eyes.

### Restoration of photoreceptor function in dogs homozygous for mutant *RPE65*

ERGs performed 5 weeks post-injection revealed reversal of photoreceptor deficits in the subretinally injected eyes (Figures 4 and 5a). There was no reversal of rod and cone function in the intravitreally injected eye or in the eyes of an affected dog that had not been treated. Waveforms developed at low-intensity light exposures.

Importantly, subretinal delivery of AAV2.*RPE65* in all three dogs resulted in ERG “a waves”, which directly reflect photoreceptor function (Figures 4 and 5). The restored “a waves” have identical timing characteristics as those in waveforms

**Table 1** Injection scheme for treated *RPE65* mutant dogs

Animal #	Left eye	PF68	Right eye	PF68	Nystagmus prior to treatment	Time after treatment until termination
BR329	SR	-	SR	+	-	5 weeks
BR334	SR	-	IV	+	+	3 months
BR332	SR	+	SR (nasal)	+	-	3 months

All eyes were injected with 150  $\mu$ l containing  $8.25 \times 10^{10}$  vector genome (vg) of AAV2.*RPE65* plus excipient in the presence (+) or absence (-) of 0.001% Pluronic F68 (PF68). All eyes injected subretinally were treated in the superior retina except for one, which was treated in the nasal retina, SR (nasal); IV (intravitreal).

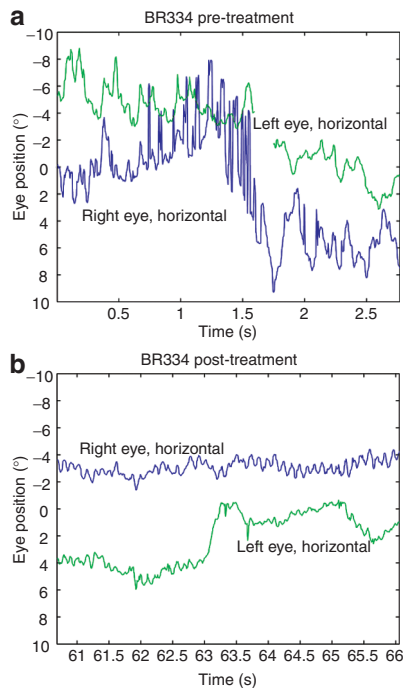


**Figure 3** Nystagmus wave forms of both eyes of dog BR334 (**a**) before and (**b**) 4 weeks after subretinal injection in the left eye. **a** Nystagmus is present in both eyes with comparable characteristics, consisting of a large amplitude ( $\sim 4^\circ$  peak-to-peak, p-p), lower-frequency ( $\sim 3$  Hz) predominantly jerk waveform combined with a smaller amplitude ( $\sim 1\text{--}2^\circ$  p-p), high-frequency ( $\sim 10$  Hz) pendular oscillation. **b** One month post-treatment, the jerk component has been eliminated, leaving only the underlying pendular oscillation. At times, the amplitude of the nystagmus in the left (subretinally injected) eye is approximately half of that in the right eye. This study presents additional evidence of the strong yoking between the movements of the two eyes, with smooth pursuit having dominance over nystagmus.

of phenotypically normal dogs (**Figure 5a**). As previously reported,<sup>8</sup> intravitreal delivery of AAV2.*RPE65* does not restore “a waves”. The “b waves,” indicative of the response of secondary retinal neurons, were also improved in subretinally treated eyes compared with baseline. Strong b waves were observed in four of the five eyes treated with subretinal AAV.*RPE65*. The amplitudes of “a waves” in eyes treated with subretinal AAV.*RPE65* were increased to 26–60% of normal (*i.e.*, those in M580) (**Supplementary Table S1**) and probably reflect the extent of retina transduced by the vector<sup>7,8</sup> (see also **Figure 1**). Amplitudes were similar to those recorded in our previous studies of treated affected dogs several months after injection.<sup>7,8</sup> Notably, the maximal a- and b-wave amplitudes of BR33 (aka Lancelot) were similar at 3 months after treatment to those in the 3-month measurements from eyes/animals treated here (**Supplementary Table S1** and **Figure 5b**),<sup>8</sup> even though Lancelot was treated with canine *RPE65* cDNA,<sup>8</sup> rather than the human *RPE65* cDNA used in this study. An unexpected finding was that amplitudes measured soon (5 weeks) after injection generally decreased by the 3-month timepoint (**Supplementary Table S1** and **Figure 4**). They were, however, still significantly larger than those in eyes of untreated affected animals, and similar to those recorded 1, 2, and 3 years after treatment for BR33 (Lancelot; **Supplementary Table S1** and **Figure 5b**).<sup>7</sup>

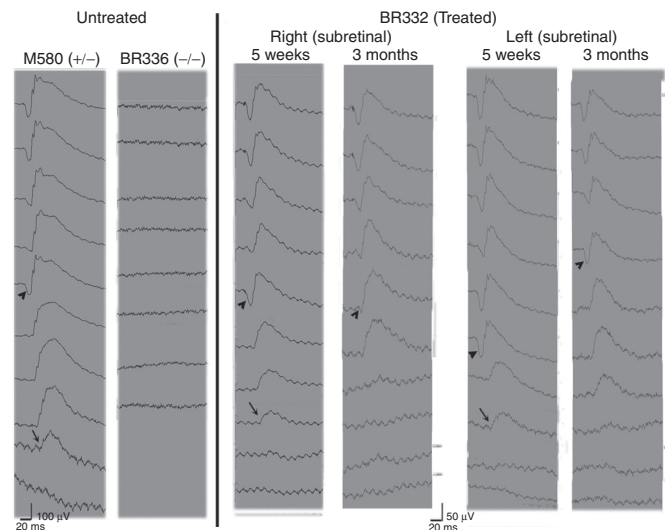


**Figure 4** Electroretinogram responses in a phenotypically normal dog; an untreated *RPE65* mutant dog (BR336) and at the 5-week and 3-month timepoints after bilateral subretinal injections in an affected dog (BR332). Waveforms developing after exposure to a light intensity series ranging from 0.000577 to 10.26 cd.s/m<sup>2</sup> (from the bottom to the top of the series) are shown. Note the waveforms present in the third to lowest light intensity of both eyes in BR332 at the 5-week timepoint as compared with the control animal M580 where a waveform developed at the second to lowest light intensity. Arrows, waveform developing at lowest light intensity. Arrowheads, the first appearance of a photoreceptor “a-wave” in the light intensity series.

Several other factors with potential influence on the amplitudes of the observed therapeutic responses were considered. The best ERG responses were found in eyes injected subretinally with AAV2.*RPE65* containing PF68 (both eyes of BR332), suggesting improved vector delivery in the presence of surfactant. BR332 right had a small intravitreal hemorrhage at the time of injection but displayed a strong ERG response despite this complication. ERG characteristics in both eyes of BR332 were similar after treatment even though the left eye received a subretinal injection in the superior retina whereas the right eye received injection in the nasal retina (**Table 1**, **Supplementary Table S1**, **Supplementary Figure S1**).

### Transgene expression and histopathology

Retinal injection sites could be identified in fixed eyecups by appearance of a “watermark” around the original site of the bleb. In some cases, folds were apparent where the retina had not completely re-aligned with the underlying rpe during re-apposition (flattening) after the subretinal injection. **Figure 6** shows ripples in the original detachment site in BR332 Right (**Figure 6f**) and large ripples in the superior center of BR334 Left (**Figure 6g**), corresponding to the original detachment sites.

Histopathological analyses in samples evaluated at both 5 weeks and 3 months revealed mostly normal retinal histology (**Figure 6a**) with baseline abnormalities consistent with *RPE65* deficiency.<sup>4,9</sup> These lesions include rpe vacuolation, rpe pigment clumping, rpe atrophy and hypertrophy, subretinal microgliosis, and modest multifocal atrophy of the outer nuclear layer (**Figure 6c**). Abnormalities due to the surgery could be identified

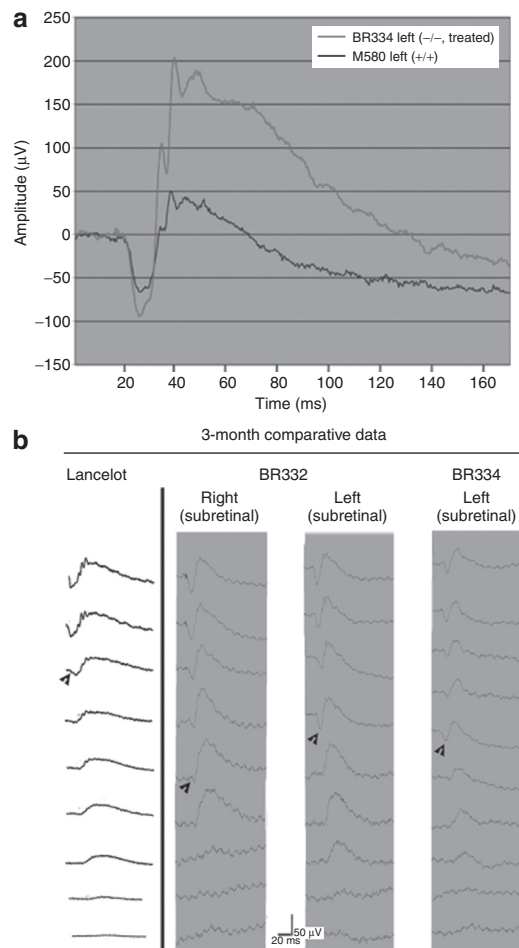


**Figure 5** Timecourse and amplitudes of electroretinograms (ERGs) in treated and control dogs. **(a)** Same timing of ERG responses in eyes of a phenotypically normal dog (M580) and an affected dog (BR334 left) injected subretinally with AAV2.RPE65. The waveform for BR334 is shown at the 5-week timepoint; **(b)** Comparison of ERGs at 3 months after injection between Lancelot (BR33)<sup>8</sup>, and BR332 and BR334. Note that the amplitudes, waveforms, and timecourse of the waveforms are similar between Lancelot and the subretinally injected eyes of BR332 and BR334. Photoreceptor response is more sensitive in BR332 OU and BR334 left as judged by the presence of a waves (arrowheads) after a stimulus of lower light intensity than resulted in “a waves” in Lancelot. The “a waves” in BR332 also have larger amplitude than those in Lancelot (after they were elicited at identical light intensities).

in those eyes that were injected subretinally (**Figure 6b**). In areas, there was loss of rpe, hypertrophy of melanocytes and rpe cells (**Figure 6b** and **c**), adhesion to the underlying choroid, and outpocketing of the neural retina from the underlying rpe (**Figure 6d**). Those lesions appeared to be a response to trauma and/or abnormal realignment of the neural retina with the underlying rpe. There was no evidence of inflammation, even in the eye that had manifested an intravitreal hemorrhage (BR332 right). Treated areas showed excellent preservation of the outer nuclear layer and of photoreceptor outer segments (**Figure 6a,b,d**).

Immunohistochemistry showed that RPE65 protein was localized to the rpe only in the region that had been exposed to virus (**Supplementary Figure S3a,b,g**), similar to what we have previously reported.<sup>7</sup> There was only minimal exposure to the

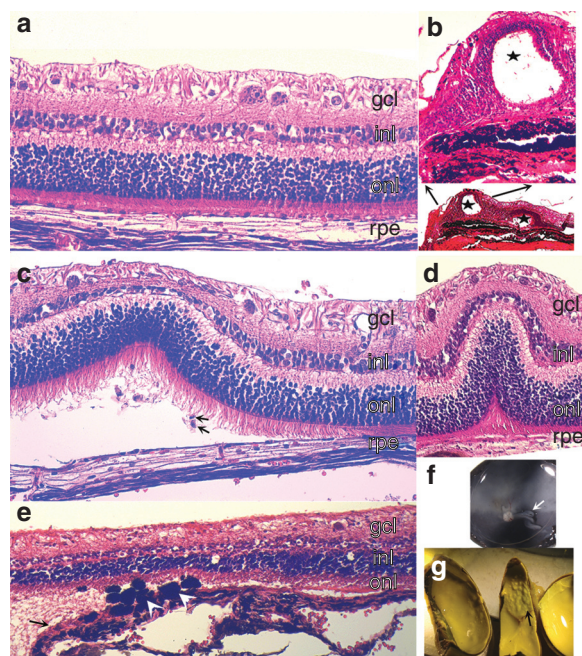


**Figure 6** Minimal histopathological changes are identified after subretinal injection of AAV2-RPE65. **(a)** In the majority of the treated retinas, cell layers [ganglion cell layer (gcl) inner nuclear layer (inl), and outer nuclear layer (onl)] are of normal thickness and retinal pigment epithelium (rpe) appears normal. Focal abnormalities in these injected eyes include: **(b)** healed retinotomy sites (one per eye) which are characterized by a transretinal defect (apparent at the left of the lower panel) and, occasionally, cystic structures (stars) in the adjacent neural retina. Arrows from the low magnification view in the lower panel indicate the region shown at higher magnification in the upper panel; **(c)** focal detachment with subretinal microglia (arrows); **(d)** focal defects in reattachment of the neural retina with resultant outpocketing of this tissue; **(e)** lesions characteristic of RPE65 deficiency, including multifocal rpe atrophy (thin arrow), rpe hypertrophy (arrowheads), and atrophy of the overlying photoreceptor layer (resulting in a thinned onl). Lesions such as those identified histologically in **c** and **d** correlated with **(f, g)** retinal folds visible in retinal eyecups prior to sectioning. Arrows in **f, g** indicate “ripples” where the neural retina had not reapposed completely to the underlying rpe.

RPE65 protein in optic nerves (**Supplementary Figure S3c**), optic chiasmata (**Supplementary Figure S3d–f**), or the brain of those animals injected subretinally.

### Immune responses

Enzyme-linked immunosorbent assay was performed to evaluate potential immune responses to both RPE65 protein and to AAV2 capsid in serum samples. None of the anterior chamber fluid or serum samples exhibited reactivity specific to RPE65 protein (data not shown). On the other hand, enzyme-linked immunosorbent assay using intact AAV2 particles as the test antigen indicated that all three of the dogs developed humoral antibodies to the AAV2 capsid by the 5-week timepoint. However, there was no detectable response at 12 weeks in the two animals for which samples were collected (**Supplementary Table S2**). In addition, there was no detectable humoral response to AAV2 capsid in anterior chamber fluid samples from eyes at the 5 or 12-week timepoints (data not shown).

Presence and levels of neutralizing antibodies were evaluated by testing the ability of different dilutions of serum to inhibit

**Table 2** Percent enhanced green fluorescent protein (eGFP) expression by 84–31 cells in the presence of serum samples from AAVRPE65-treated Briard dogs

Serum dilution	BR329 baseline	BR329 5 weeks	BR332 baseline	BR332 5 weeks	BR332 3 months	BR334 baseline	BR334 5 weeks	BR334 3 months
1:5	94 ± 10	<b>6 ± 1</b>	93 ± 5	5 ± 2	5 ± 2	107 ± 26	4 ± 2	<b>3 ± 0</b>
1:10	104 ± 6	<b>6 ± 1</b>	101 ± 4	<b>6 ± 2</b>	<b>6 ± 2</b>	113 ± 16	7 ± 5	<b>5 ± 1</b>
1:100	110 ± 13	<b>6 ± 2</b>	99 ± 10	7 ± 1	120 ± 6	106 ± 14	5 ± 2	113 ± 15
1:1,000	107 ± 4	118 ± 8	105 ± 5	<b>18 ± 4</b>	95 ± 8	102 ± 11	<b>48 ± 8</b>	98 ± 10
1:10,000	115 ± 12	98 ± 8	103 ± 8	95 ± 7	100 ± 5	103 ± 7	96 ± 3	99 ± 5

Numbers reflect the percent eGFP expression in presence of sample (mean ± SD). The percent eGFP expression in the absence of sample is 100 ± 6 ( $n = 36$ ); results indicating ≥50% inhibition are shown in boldface text.

**Table 3** Serum neutralizing antibody titers\* of AAVRPE65-treated Briard dogs

	Baseline	5 Weeks	3 Months
BR329	None detected	100	NA
BR332	None detected	1,000	10
BR334	None detected	1,000	10

\*Titer is the reciprocal of the highest dilution that results in <50% enhanced green fluorescent protein (eGFP) expression as compared to control; NA, not available.

transduction by AAV2/2.CMV.eGFP *in vitro* in 84–31 (kidney) cells. Results for the serum samples showed no inhibition of enhanced green fluorescent protein expression by any of the baseline serum samples; while all post-treatment samples exhibited some inhibitory activity (Table 2). As shown in Table 3, neutralizing antibodies to AAV2 capsid were detectable at a titer of 1,000 in two animals 5 weeks after treatment but decreased to 10 at the 3-month timepoint. Anterior chamber fluid collected at necropsy had low titers of neutralizing antibodies 3 months after treatment.

### Enzyme-linked immunosorbent assay

Enzyme-linked immunosorbent (enzyme-linked immunosorbent spot) assay was used to evaluate potential cellular immune responses directed to AAV2 capsid antigen. At 12 weeks, there were no detectable T-cell responses in animals (BR332 and BR334) that were exposed intraocularly to AAV2.RPE65 (Supplementary Figure S4).

## DISCUSSION

This study demonstrates that subretinally delivered recombinant AAV2 carrying CBA-driven wild-type *hRPE65* cDNA, can restore retinal function in Rpe65 mutant mice, that have heretofore been refractory to treatment with AAV2. In addition, the study confirms and expands upon our previous finding that a single dose of subretinally delivered AAV2.RPE65 can restore vision in the canine model of RPE65-associated LCA. The rpe cells in the targeted region expressed RPE65 protein, completing the biochemical circuit necessary for the retina to produce 11-*cis*-retinal and to regenerate rhodopsin. Recovery of visual function was dramatic and was evident within 2 weeks of treatment in dogs. In previous studies, the earliest measurements showing reversal of vision (ERG recordings) were made at 2.75–3 months after subretinal injection of AAV2.RPE65.<sup>7,8,12,13,16</sup> There are no other reports of improvement of retinal/visual

function so soon after injection. Here, the earliest signs of recovery were improved pupillary light responses and reduced nystagmus. Similar to what we reported previously in affected dogs evaluated 8–23 months after subretinal injection, nystagmus was improved in both eyes in the dog that had received unilateral subretinal injection.<sup>17</sup> Diminution of nystagmus is conducive to improved visual acuity, because fixation targets better remain within the extent of the area centralis (+3° horizontal).

Improvements in our vector design and formulation likely contributed to the earlier and improved indications of efficacy as compared with previous studies.<sup>7,8</sup> Incorporation of appropriate *cis*-regulatory sequences and addition of a modified Kozak sequence at the translational start site of *hRPE65* optimized expression and production of the transgenic RPE65 protein. However, since the preparations used in previous studies differ in many ways (including AAV serotype, source of cDNA, regulatory sequences, purification, diluent, dose administered) from that used in this study, it is not possible to make a direct comparison between these vectors.

Vector generation and purification procedures minimized dilution of the reagent with empty AAV capsids, which could potentially engender an immune response without delivering the therapeutic transgene. After treatment, we identified small and transient increases in humoral (but not intraocular) anti-AAV2 capsid antibodies and also generation of neutralizing antibodies. This is the first time that such a response has been reported after subretinal injection of AAV. Further studies will evaluate the significance and relevance of these antibodies with respect to readministration of the vector. There was no evidence of generation of a cellular immune response to AAV2. Such responses would potentially be the most serious complication with respect to readministration.

While ERG amplitudes decreased in some of the eyes between the 5-week and 3-month timepoints, animals continued to enjoy vision through termination of the study and there were no signs of inflammation upon clinical exam or at necropsy. The significance of the early decrease in ERG amplitudes is unknown since there are no other reports of serial measurements soon after treatment. The only serial measurements available are those from animals followed long term (over years). In BR33 (Lancelot), amplitudes varied by <10% over a 3-year interval (Supplementary Table S1).<sup>7</sup>

Perhaps the most dramatic improvement with respect to delivery of the AAV was due to the addition of a low concentration of surfactant to the vehicle. Without surfactant, up to 75% of the vector was lost to inert surfaces, significantly reducing the dose

of vector delivered. In this study, we developed an approach that allows consistent and predictable delivery of a given dose of vector. Although this study was not designed to determine whether co-injection of AAV2.*RPE65* and PF68 enhances recovery of vision over injection of AAV2.*RPE65* alone, the strongest therapeutic effects were identified in eyes treated subretinally with AAV2.*RPE65* plus PF68, suggesting that they received a larger therapeutic dose. PF68 is a non-ionic surfactant that has been approved for human use by the Food and Drug Administration and has already been delivered in conjunction with AAV in a Phase I/II clinical trial for Parkinson's disease (JBB-IND-11366). In this ongoing study, five subjects have received intracranial (striatal) injection of vector, and results have demonstrated excellent safety (John Forsayeth, University of California, San Francisco, personal communication, 8 June 2007). Improved precision in the control of the surgically delivered dose will be an important contribution in minimizing the variables affecting safety and therapeutic efficacy in animals and ultimately, in humans treated with AAV vectors. In the studies described here, PF68 appeared safe locally and systemically. Data from additional large animal studies, also support safety of delivery of PF68 to the retina (Bennett, *et al.*, unpublished result).

In summary, our AAV2.*RPE65* virus and formulation have improved features compared with previous vectors/formulations. No significant inflammatory or other deleterious effects of the therapy have been observed. The data demonstrate that AAV.*RPE65* delivers the *RPE65* transgene efficiently, quickly, and stably to rpe cells *in vivo* in animal models, resulting in a therapeutic effect evident within weeks of treatment with minimal toxicity. This vector holds great promise for treatment of LCA due to *RPE65* mutations.

## MATERIALS AND METHODS

**Vector.** The *cis* plasmid used to generate AAV2.*RPE65* contains the kanamycin-resistance gene, and the transgene expression cassette contains a hybrid CBA promoter comprising the cytomegalovirus immediate early enhancer (0.36 kb), the proximal CBA promoter (0.28 kb), and CBA exon 1 flanked by intron 1 sequences (0.997 kb). To include a Kozak consensus sequence at the translational start site, the sequence surrounding the initiation codon was modified from GCCGCATGT in the original vector to CCACCATGT. The virus was manufactured by The Center for Cellular and Molecular Therapeutics after triple transfection of HEK293 cells and was isolated and purified by microfluidization, filtration, cation-exchange chromatography (POROS 50HS; GE Healthcare, Piscataway, NJ), density gradient ultracentrifugation and diafiltration in PBS. This combination provides optimal purity of the AAV vector product, including efficient removal of empty capsids and residual cesium chloride. A portion of the product was supplemented with PF68 NF Prill Poloxamer 188 (PF68; BASF, Ludwigshafen, Germany) to prevent subsequent losses of vector to product contact surfaces. The purified virus, with or without PF68, was then passed through a 0.22- $\mu$ m filter using a sterile 60-ml syringe and syringe filter, and stored frozen ( $-80^{\circ}\text{C}$ ) in sterile tubes until use. Quality control procedures performed to characterize the vector included real-time quantitative polymerase chain reaction (to assess vector genome concentration), sodium dodecyl sulfate-polyacrylamide gel electrophoresis and silver staining (for vector purity), osmolality, pH, and endotoxin testing (see **Supplementary Methods S1**).

### Animals.

**Mice:** All procedures involving animals were undertaken in accordance with local and federal guidelines on Humane Care and Use of

Laboratory Animals. *Rpe65* knockout mice<sup>11</sup> were generously provided by T.M. Redmond (Laboratory of Retinal Cell and Molecular Biology, National Eye Institute, National Institutes of Health, Bethesda, MD, USA). *Rd12* (spontaneous *Rpe65* mutant) mice were from Jackson Labs (Bar Harbor, ME). Subretinal injections were performed as previously described.<sup>15,18,19</sup> Abbreviated ERGs were performed using photopic and scotopic conditions as described.<sup>15,17,20,21</sup> The rod  $b_{\max}$  was determined by  $<100\text{-}\mu\text{s}$  flashes of  $0.02\text{-scot cd m}^{-2}$  intensity white light. The  $a_{\max}$  was determined by  $300\text{-}\mu\text{s}$  flashes of  $200\text{-scot cd m}^{-2}$  intensity white light. The threshold intensity to evoke a criterion ( $20\mu\text{V}$ ) ERG b-wave response was determined by plotting b-wave amplitudes (measured conventionally from baseline or a-wave trough to positive peak). The visual acuity in experimental and control eyes of four *rd12* mice was measured using optomotor responses to a rotating sine-wave grating (CerebralMechanics OptoMotry system, Alberta, Canada).<sup>22,23</sup> *RPE65* immunohistochemistry was performed after fixation and cryosectioning<sup>15</sup> using a rabbit anti-mouse *RPE65* polyclonal antibody (PETLET, gift of Dr. T.M. Redmond) and 4,6-diamidino-2-phenylindole nuclear stain.

**Dogs:** The three dogs treated in this study (identified as BR329, BR332, and BR334) were homozygous for the 4-basepair deletion in the canine *RPE65* gene<sup>10</sup> and were obtained from the Retinal Disease Studies Facility, Kennett Square, PA. In addition, two eyes each from a control dog heterozygous for the *RPE65* mutation (M580) and from an untreated affected dog (BR336) were used for ERG studies. Subretinal injections were performed as described after performing an anterior chamber paracentesis.<sup>7,8,24</sup> A vector dose of  $8.25 \times 10^{10}$  vg in a volume of  $150\mu\text{l}$  was delivered, thereby creating a localized dome-shaped retinal detachment. Ocular motility studies were performed using methods previously described by Jacobs *et al.* 2006.<sup>17</sup>

**ERG.** Dogs were dark-adapted and ERGs were performed under general anesthesia.<sup>7,8</sup> Full-field ERGs were recorded with Burian-Allen contact lens electrodes and a computer-based system. Low-energy (4-ms duration; maximum luminance of unattenuated white flash =  $1.0 \log \text{scot-cd.s.m}^{-2}$  or  $10.26 \text{cd.s.m}^{-2}$ ) flashes were used under dark-adapted and light-adapted ( $30 \text{cd.m}^{-2}$  at 1 Hz stimulation,  $10 \text{cd.m}^{-2}$  at 29 Hz stimulation) conditions.

**Histopathology, Immunocytochemistry.** Retinal sections for morphologic studies were prepared using either a triple fixation protocol<sup>7,8</sup> prior to embedding in paraffin, or 4% paraformaldehyde fixation for cryosectioning and immunocytochemistry. Tissues were oriented such that the sections extended through the center of the treated area; non-treated areas from adjoining and other quadrants were also included for analysis. Immunohistochemistry used an anti-mouse *RPE65* polyclonal antibody (see above), 4,6-diamidino-2-phenylindole nuclear stain, and/or peanut agglutinin lectin to label the insoluble extracellular domain surrounding cone photoreceptors. Secondary antibodies included goat anti-rabbit immunoglobulin G conjugated to either Alexa Fluor 488 (green) or Alexa Fluor 568 (red; Molecular Probes-Invitrogen, Carlsbad, CA). Sections were examined with a Leica DMRE microscope using epifluorescence and DIC optics (Leica Microsystems, Deerfield, IL). Images were digitally captured with a Hamamatsu digital camera and OpenLab 4.0 Image Analysis Software (Improvision, Boston, MA), and imported into Adobe Photoshop (Adobe Systems, San Jose, CA).

**Samples for serology, virology, and extraocular transgene expression.** Serum samples were obtained by venipuncture on the day of subretinal injection (baseline), 5 weeks after injection (BR329 necropsy timepoint as well), and again, terminally at 10.5 weeks (BR332 and BR334). Anterior chamber fluids were collected at baseline. Following killing, eyes that were enucleated for other studies and fluid samples collected from the anterior chamber and vitreous. All samples were stored at  $-80^{\circ}\text{C}$  until used for immunology studies (see **Supplementary Methods S2**).

## ACKNOWLEDGMENTS

Supported by the National Institutes of Health (EY10820; EY06855; EY015398); The Center for Cellular and Molecular Therapeutics/Children's Hospital of Philadelphia, The Foundation Fighting Blindness; Research to Prevent Blindness; F.M. Kirby Foundation and Macula Vision Research Foundation. We are especially grateful to Jennifer McDonnell and Junwei Sun for helpful discussions and extraordinary support. Technical assistance from Amanda Nickle, Gerri Antonini, Tracy Greiner, Alice Eidsen, and the staff at the Retinal Disease Studies Facility is gratefully acknowledged. We thank Edward Pugh, Jr. for his expertise and advice on ERG analysis in dogs, and Arkady Lyubarsky for his expertise and assistance with ERGs in mice (both from Scheie Eye Institute, University of Pennsylvania, Philadelphia, PA) A.M.M. and J.B. are listed as co-authors on a patent application entitled "Method of treating or retarding blindness"; however, both individuals waived any financial gain in 2002.

## SUPPLEMENTARY MATERIAL

**Figure S1.** Montages of representative fundus views immediately after subretinal (BR329 and BR332 both eyes and BR334 left eye) or intravitreal (BR334 right eye) injection.

**Figure S2.** Afferent pupillary responses 2 weeks after treatment of BR334.

**Table S1.** Amplitudes of a-max and b-max in dogs studied here and in the treated eye of BR33 (aka Lancelot).<sup>1,2</sup>

**Figure S3.** RPE65 protein is detectable by immunohistochemistry in the (a, b, g) injection sites of dog retinas treated with AAV2.RPE65 but (h) not in adjacent untreated retina.

**Table S2.** Humoral Immune responses to AAV2 capsid protein, 3 weeks and 3 months after injection.

**Figure S4.** ELISpot analysis reveals no evidence of T cell responses to the AAV2 capsid after subretinal or intravitreal injection with AAV2.RPE65.

**Materials and methods S1.**

**Materials and methods S2.**

## REFERENCES

- Hanein, S, Perrault, I, Gerber, SA, Tanguy, G, Barget, F, Ducroz, D *et al.* (2004). Leber congenital amaurosis: comprehensive survey of the genetic heterogeneity, refinement of the clinical definition, and genotype-phenotype correlations as a strategy for molecular diagnosis. *Hum Mut* **23**: 306–317.
- Cremers, FP, van den Hurk, JA and den Hollander, AI (2002). Molecular genetics of Leber congenital amaurosis. *Hum Mol Genet* **11**: 1169–1176.
- Thompson, D and Gal, A (2003). Vitamin A metabolism in the retinal pigment epithelium: genes, mutations, and diseases. *Prog Retin Eye Res* **22**: 683–702.
- Narfstrom, K, Wrigstad, A and Nilsson, S (1989). The Briard dogs: a new animal model of congenital stationary night blindness. *Br J Ophthalmol* **73**: 750–756.
- Pang, JJ, Chang, B, Hawes, NL, Hurd, RE, Davisson, MT, Li, J *et al.* (2005). Retinal degeneration 12 (rd12): a new, spontaneously arising mouse model for human Leber congenital amaurosis (LCA). *Mol Vis* **11**: 152–162.
- den Hollander, A, Koeneke, RK, Mohamed, MD, Arts, HH, Boldt, K, Towns, KV *et al.* (2007). Mutations in *LCA5*, encoding the novel ciliary protein lebercilin, cause Leber congenital amaurosis. *Nat Genet* **39**: 889–895.
- Acland, GM, Aguirre, GD, Bennett, J, Aleman, TS, Cideciyan, AV, Bencicelli, J *et al.* (2005). Long-term restoration of rod and cone vision by single dose rAAV-mediated gene transfer to the retina in a canine model of childhood blindness. *Mol Ther* **12**: 1072–1082.
- Acland, GM, Aguirre, GD, Ray, J, Zhang, Q, Aleman, TS, Cideciyan, AV *et al.* (2001). Gene therapy restores vision in a canine model of childhood blindness. *Nat Genet* **28**: 92–95.
- Aguirre, G, Baldwin, V, Pearce-Kelling, S, Narfstrom, K, Ray, K and Acland, G (1998). Congenital stationary night blindness in the dog: common mutation in the RPE65 gene indicates founder effect. *Mol Vis* **4**: 23.
- Veske, A, Nilsson, S, Narfstrom, K and Gal, A (1999). Retinal dystrophy of Swedish Briard/Briard-Beagle dogs is due to a 4-bp deletion in RPE65. *Genomics* **57**: 57–61.
- Redmond, TM and Hamel, CP (2000). Genetic analysis of RPE65: from human disease to mouse model. *Methods Enzymol* **316**: 705–724.
- Narfstrom, K, Katz, ML, Bragadottir, R, Seeliger, M, Boulanger, A, Redmond, TM *et al.* (2003). Functional and structural recovery of the retina after gene therapy in the RPE65 null mutation dog. *Invest Ophthalmol Vis Sci* **44**: 1663–1672.
- Narfstrom, K, Katz, ML, Ford, M, Redmond, TM, Rakoczy, E and Bragadottir, R (2003). *In vivo* gene therapy in young and adult RPE65<sup>-/-</sup> dogs produces long-term visual improvement. *J Hered* **94**: 31–37.
- Lai, CM, Yu, MJ, Brankov, M, Barnett, NL, Zhou, X, Redmond, TM *et al.* (2004). Recombinant adeno-associated virus type 2-mediated gene delivery into the Rpe65<sup>-/-</sup> knockout mouse eye results in limited rescue. *Genet Vaccines Ther* **2**: 3.
- Dejneka, NS, Surace, EM, Aleman, TS, Cideciyan, ZV, Lyubarsky, A, Savchenko, A *et al.* (2004). *In utero* gene therapy rescues vision in a murine model of congenital blindness. *Mol Ther* **9**: 182–188.
- Ford, M, Bragadottir, R, Rakoczy, PE and Narfstrom, K (2003). Gene transfer in the RPE65 null mutation dog: relationship between construct volume, visual behavior and electroretinographic (ERG) results. *Doc Ophthalmol* **107**: 79–86.
- Jacobs, J, Dell'Osso, L, Hertle, R, Acland, G and Bennett, J (2006). Eye movement recordings as an effectiveness indicator of gene therapy in RPE65-deficient canines: implications for the ocular motor system. *Invest Ophthalmol Vis Sci* **47**: 2865–2875.
- Bennett, J, Duan, D, Engelhardt, JF and Maguire, AM (1997). Real-time, noninvasive *in vivo* assessment of adeno-associated virus-mediated retinal transduction. *Invest Ophthalmol Vis Sci* **38**: 2857–2863.
- Liang, F-Q, Anand, V, Maguire, AM and Bennett, J (2000). Intraocular delivery of recombinant virus. In: Rakoczy, PE (ed.) *Methods in Molecular Medicine: Ocular Molecular Biology Protocols*. Humana Press Inc: Totowa, NJ. pp. 125–139.
- Lyubarsky, AL and Pugh, EN, Jr (1996). Recovery phase of the murine rod photoreceptor reconstructed from electroretinographic recordings. *J Neurosci* **16**: 563–571.
- Lyubarsky, AL, Falsini, B, Pennesi, ME, Valentini, P and Pugh, EN, Jr (1999). UV- and midwave-sensitive cone-driven retinal responses of the mouse: a possible phenotype for coexpression of cone photopigments. *J Neurosci* **19**: 442–455.
- Douglas, RM, Alam, NM, Silver, BD, McGill, TJ, Tschetter, WW and Prusky, GT (2005). Independent visual threshold measurements in the two eyes of freely moving rats and mice using a virtual-reality optokinetic system. *Visual neurosci* **22**: 677–684.
- Umino, Y, Everhart, D, Solessio, E, Cusato, K, Pan, JC, Nguyen, TH *et al.* (2006). Hypoglycemia leads to age-related loss of vision. *Proc Natl Acad Sci* **103**: 19541–19545.
- Bennett, J, Anand, V, Acland, GM and Maguire, AM (2000). Cross-species comparison of *in vivo* reporter gene expression after recombinant adeno-associated virus-mediated retinal transduction. *Methods Enzymol* **316**: 777–789.